Effect of hygrothermal ageing on the shear creep behaviour of eco-friendly sandwich cores

Authors: Benjamin Sala[*1], Xavier Gabrion[1], Thomas Jeannin[1], Frédérique Trivaudey[1], Violaine Guicheret-Retel[1], Fabrizio Scarpa[2], Vincent Placet[1]

Affiliation : [1]Univ. Bourgogne Franche-Comté, FEMTO-ST Institute, UFC/CNRS/ENSMM/UTBM, Department of Applied Mechanics, F-25000 Besançon.

[2]Bristol Composites Institute (ACCIS), University of Bristol, BS8 1 T, UKR, Bristol, UK

Abstract:

The development of sustainable sandwich materials is needed in the transportation sector to address environmental concerns related to the production and operation of vehicles. In addition to biobased composite skins, alternatives to classic synthetic core materials must be found to reduce the ecological footprint of whole sandwich-structured composites. This study focused on three eco-friendly lightweight core materials: balsa wood, paper honeycomb, and recycled PET foam. The effect of the hygrothermal ageing on their shear creep/recovery behaviour has been here investigated. Two different environmental conditions were tested: 23 °C-50% RH and 70 °C-65% RH. The results indicate that the maximum shear strain, the time-delayed strain and the residual strain increase for the three core materials with the severity of the hygrothermal conditions. This was attributed to the softening of the constitutive polymeric materials of the cell walls at temperatures close to 70 °C. The balsa wood exhibits the best creep resistance under the two environmental conditions. The identification of the viscoelastic properties highlights that the release times and the shear viscous parameter of the balsa wood and the PET foam depended on the stress level and the hygrothermal conditions.

Keywords: sandwich core, eco-friendly, creep/recovery, hygrothermal environment

1. INTRODUCTION

A sandwich-structured composite consists of two stiff composite skins bonded to a low-strength and lightweight core material [1]. It is generally designed to produce panels with high bending stiffness with an overall low specific weight. Sandwich composites are commonly used in various applications, such as aeronautical, automotive, and civil engineering [2,3]. Under bending, the core material is subjected to shear stress. Therefore, the selection of the core material is mainly based on lightness and transverse shear performance. The most common and commercially available cores are foams such as polyurethane (PU) and polyvinyl chloride (PVC), balsa wood (Ochroma pyramidale), and honeycombs (made of paper, aluminium or aramid) [4,5]. To address global concerns

over environmental issues and to ensure an ecological transition towards a sustainable development of various industrial sectors, more environmentally friendly sandwich materials are required. Recent studies have focused on plant fibre composites [6–8] and biobased and/or recycled materials for cores [9–14]. New classes of biobased materials can represent an alternative to traditional fossil constituents and reduce carbon and more general environmental footprints. The transition to more environmentally friendly sandwich materials begins with the selection of lightweight biobased or recycled materials with high shear properties. Most biobased materials are also more sensitive to temperature and moisture than the majority of the traditional synthetic ones, and also require a thorough investigation of their mechanical performance, in particular their creep behaviour in various and changing environments to which sandwich materials are often submitted in service conditions.

Three eco-friendly materials have been selected in this study to evaluate their potential as cores in sustainable sandwich materials: reconstituted balsa wood panels, paper honeycombs, and recycled polyethylene terephthalate (rPET) foam. Balsa wood panels were selected because they are made from natural and renewable resources that are light and available. Balsa is a medium-sized fast-growing pioneer subtropical and tropical tree (typically reaching 25 m in height and 1 m in diameter) that is deciduous or evergreen and occurs in both pure and mixed stands in association with other pioneer species [15]. Balsa is not a tree in danger of extinction due to its fast growth and ease of reproduction. It is cultivated on plantations during 5–7-year rotations, primarily in the South American country of Ecuador. Its production, reaching 18 000 ha in 2008 in Ecuador, contributes to the economy of the country [16]. Due to its rapid growth, balsa wood also has a relatively low density compared to other wood species [15]. The density of dry balsa wood ranges from 60 to 380 $kg.m^{-3}$ [17]. Ecuador's environment, altitude, and climate offer stable wood in terms of density. Additionally, during photosynthesis, some atmospheric CO_2 is stored in the wood, approximately 1.81 kg of CO_2 per kg of balsa wood [13]. Balsa also improves soil fertility [18]. For application as a core in sandwich panels, balsa wood often comes in the form of reconstituted wood blocks bonded with a polyvinyl alcohol (PVA) adhesive. To produce 1 kg of balsa wood panel, approximately 4 kg of balsa trunks are needed [13].

Paper honeycombs were also selected as a biobased material with a high mechanical performance to weight ratio, surpassing bulk wood cores [19]. Additionally, paper honeycombs are a low-cost material [20]. In the construction field, cardboard honeycombs are increasingly used as insulation materials, as a substitution for polyurethane foam or glass wool [21]. Paper pulp is extracted from raw material using mechanical or chemical processes. To produce one tonne of pulp, 3 and 1.1 tonnes of wood are necessary using the abovementioned processes, respectively. Energy consumption accounts for approximately 16% of the total production costs of the pulp and paper [22].

Cardboard is 13% less energy intensive than steel [23]. According to a report from the Confederation of European Paper Industries [24], the energy consumed to produce pulp and paper is based on biomass. A total of 1.05 MWh are needed to produce 1 tonne of product. Additionally, the direct CO_2 emissions per kilotonne of product are equal at 0.34 kt.

The last type of core considered in this work was a foam made of recycled polyethylene terephthalate (PET) from water bottles. The amount of plastic waste is worldwide increasing. Between 2006 and 2016 in Europe only, plastic waste collection has increased by 11% from 24.5 million tonnes to 27.1 million tonnes [25]. This waste can have a detrimental effect on the environment, hence the necessity to recycle this material [26]. The recycling rate for plastic packaging was 40.8% in Europe with a target of 50% by 2025 [25]. Therefore, recycling water bottles into a PET foam helps to reduce the impact of plastic waste on the environment. In addition, according to Armacell's life cycle assessment [27], the production of the recycled PET foam allows having an environmental carbon footprint 49% lower than producing a virgin PET foam. However, for a same density and according to the technical data sheets, the shear modulus of the recycled PET foam is approximatively 30% lower than that of the virgin PET foam (AIREX T92.80) [28,29].

In addition to their eco-friendliness, materials selected as constituents for a sandwich panel must also possess high shear mechanical properties. To accurately predict and understand the mechanical response at the sandwich scale, in-depth knowledge of the mechanical behaviour of the composite skins and of the core materials is required. For this work realized in the framework of the European project SSUCHY (https://www.ssuchy.eu/), the targeted application concerns the floor and trim panel structures for automotive sector, which requires long-term durability, particularly under varying hygrothermal conditions.

The quasi-static shear behaviour of the three selected cores has already been investigated in open literature. The shear behaviour of balsa wood is particularly well documented. Concerning balsa samples extracted from blocks of the reconstituted balsa panel, studies have highlighted a linear dependence of the shear modulus and shear ultimate stress on the density of the wood [30–32]. The presence of the adhesive between the blocks of the reconstituted balsa core tends to stiffen the material and improve its strength [30]. Garrido *et al.* [33] carried out an experimental campaign on balsa samples for a range of temperatures between 23 °C and 240 °C. The authors observed a degradation of the mechanical properties with increasing temperature. The influence of water immersion on the mechanical properties of the balsa was only studied under compression [34]. The experimental results highlight a decrease in the compression modulus, particularly during the first week of immersion. At the scale of the reconstituted balsa core, Monti [14] showed that balsa wood had a higher specific shear modulus than

PVC foam, PET foam and Kevlar honeycomb. The shear mechanical properties were also determined by Fathi *et al.* [35] using a direct shear test or by the inverse method from the strain field measured in the core material during a four-point bending test on a sandwich beam with glass fibre reinforced epoxy skin. The shear modulus and the strength were shown to be independent of the method to acquire the data. The strain at failure was however underestimated when using the direct shear measurement. The use of strain field measurements also highlighted the presence of a heterogeneous strain field in the balsa material due to the natural origin of the material. Recently, some authors have developed a veneered core made of a thin layer of reconstituted balsa [36,37]. By turning the layer orientations, the idea was to decrease the scatter of the mechanical properties and to tailor these properties to specific applications. In particular, the work of Vahedi *et al.* [37] on veneered balsa core showed a decrease in the shear modulus and strength with increasing temperature. In addition, the increase in the moisture content of the reconstituted balsa leads to a decrease in the mechanical properties such as bending or compressive modulus and ultimate stress [38,39]. The influence of water content on the shear behaviour of balsa has not yet been investigated in the literature. The quasi-static shear behaviour of balsa wood in a severe environment (high temperature and humidity level) and the time-delayed behaviour have not yet been addressed by the scientific community.

Concerning PET foams and paper honeycombs, the shear behaviour is less documented. Although some authors have used paper honeycombs as the core of sandwich panels [40–42], the main contribution was made by Pohl [43]. The author characterized the quasi-static shear behaviour of a paper honeycomb and tested paper honeycomb specimens for a long time under real environmental conditions. The measure of the relative humidity during the tests showed that summer was characterized by a mean level of relative humidity higher than that in winter. Interestingly, the shear strain rate was greater in the summer than during winter. However, the influence of a severe environment on time-delayed behaviour has not been explored.

Fathi *et al.* [35] showed that, despite the higher density, the shear modulus of PET foam was lower than that of PVC foams. The use of strain field measurements allowed to identify a more uniform distribution of the shear strain in the PET foam compared to PVC foam, also due to a more homogenous repartition of the cell sizes. Garrido *et al.* [33] loaded PET foam specimens under shear over a large temperature range (between -20 °C and 120 °C). The results showed a decrease in shear modulus with increasing temperature. Those authors demonstrated that different empirical models can accurately describe the variation in the shear modulus as a function of the temperature level. No studies however have been carried out so far on the creep behaviour of PET foams.

The aim of this study is to fill the gap in literature concerning the time-delayed shear behaviour of core materials and to evaluate the influence of hygrothermal ageing on this mechanical response. This study focuses on the quasi-static and creep/recovery shear behaviour of balsa wood, paper honeycomb, and recycled PET (rPET) foam panels. They were tested under two hygrothermal conditions, namely, 23 °C-50% relative humidity (RH), and 70 °C-65% RH. Due to the expression of an irreversible mechanism during the creep stage, under a severe environment, the viscoelastic behaviour was analysed in the recovery stage.

2. MATERIALS AND METHODS

2.1. Materials

2.1.1. Materials presentation and microstructure

Three different materials were studied in this research. Figure 1 presents them and the associated coordinate systems. The first core was the balsa wood panel Baltek SB50 from 3A Core® provided by Sicomin®. It was a 25.4 mm thick rigid panel made of blocks assembled by adhesive bonding. The blocks were cut perpendicular to the tree growth direction (end grain balsa). The length and width of the reconstituted balsa wood panel were chosen as the two main material directions (directions L and T, respectively). The second material was an expanded 8 cell size paper honeycomb provided by Axxor® company. This core is labelled as H-3D-140-1400-8.1-20.0-N-57 and a thickness of 20 mm. The L-direction was defined as the direction of the ribbon, and the T-direction was perpendicular to the L-direction. The third studied material was a recycled polyethylene terephthalate (rPET) foam ArmaPET Struct GR80 manufactured from PET bottles and provided by Armacell®. This foam has the particularity of having darker colour lines corresponding to welding lines. The material coordinate system was therefore chosen so that the L-direction was parallel to the direction of these lines and the T-direction was perpendicular to these lines. For all the core materials, the T' direction was defined as the direction perpendicular to the plane (L,T).

Microscopic observations of the core materials, carried out using a Keyence VHX5000 numerical microscope, are presented in Figure 1. The balsa wood is composed of fibres and rays. According to Borrega *et al.* [17], it represents 66% to 76% and 20% to 25% of the volume of the microstructure, respectively. Prismatic in shape and composed of thick cell walls, the fibres enable the tree to be maintained. The cell wall of the fibres is divided into 3 sublayers labelled S1, S2 and S3. The S2 layer is the thickest and is composed by cellulose microfibrils of a matrix of hemicellulose and lignin [32]. Microfibrils are made up of both amorphous and crystalline cellulose with a crystallinity index of approximately 40% [17].

The paper honeycomb consists of open hexagonal cells with a characteristic size of approximately 7 mm. Based on the microscopic observation, the thickness of the paper wall is comprised between 0.2 and 0.5 mm. The

principal constituent of the paper is cellulose fibres with lengths between 1 and 3 mm [43]. Some additives can also be used in the paper and can alter the mechanical properties of the paper.

The structure of the rPET foam made of closed hexagonal cells is also visible in Figure 1. The width of these cells is between 0.6 and 1 mm.

2.1.2 Determination of the density and moisture content at equilibrium

The equilibrium moisture content (EMC) of the three core materials was determined following the ASTM C272 standard [44] under two different environmental conditions: 23 °C-50% RH, labelled EC1, and 70 °C-65% RH, labelled EC2. A balance with an accuracy of 0.001 g was used to weight the specimens. Square section samples with 150 mm side and 25 mm thick were used for the balsa wood and square section samples with 120 mm side and 20 mm thick were used for the two other materials. The edges of the samples were not protected. All materials are first stored for a minimum of one and a half months in a room with a temperature and humidity of 23±3 °C-50±10% RH. In order to control the hygrothermal conditions more finely, the specimens were then conditioned in environment EC1 using a Memmert HPP 108L climatic chamber. Then, the climatic chamber is set to the environmental condition corresponding to the environment EC2. Finally, the cores were removed from the climatic chamber and putted into an oven at 103 °C to dry the specimens in accordance with the ASTM D4442 standard [45]. The mass of the different samples was measured after at least 20 days in EC1 (m_{EC1}), then 7 days in EC2 (m_{EC2}) and finally after drying for 7 days at 103 °C (m_{dry}). For each condition, the equilibrium was considered to be reached when the variation of mass was infinitesimal between two measuring points with time interval of 24h.

The equilibrium moisture content (MC^{ECi}) under the environmental condition ECi was calculated as follows:

$$MC^{ECi} = 100 \times \frac{m_{ECi} - m_{dry}}{m_{dry}} \quad (1)$$

The density of the core materials was measured under environment EC1. At least 10 samples with a length of 300 mm and a width of 50 mm were tested. The thicknesses of the samples were 25 mm for balsa wood and 20 mm for the other core materials.

2.2 Mechanical testing

2.2.1 Monotonic shear tests

Testing parameters

The core materials were tested under shear solicitation using an MTS® Criterion 45 machine instrumented with a 100 kN load cell. For this purpose, a shear assembly was specially designed in accordance with the ASTM C273

standard [46]. The samples are first bonded to two metal parts. One of these metal parts was then embedded in a mobile plate, while the other part was embedded in a fixed plate. Monotonic shear tests were realized in EC1 (23±3 °C-50±10% RH) and EC2 (70±3 °C-65±5% RH). To control the environment during shear testing and then maintain hygrothermal conditions similar those used during sample conditioning, a polymethyl methacrylate (PMMA) box, connected to an Inec70-90 relative humidity generator from Ineltec®, was installed on the tensile machine. Figure 2 shows the set-up. The displacement between the two metal parts was measured using an LVDT sensor with a measurement range of 10 mm. The solicitation speed was fixed at 1 mm/min. The dimensions of the samples were 50 mm in width and 300 mm in length. The thicknesses of the samples were equal to the dimensions of the initial core material panels. The shear planes (L,T') and (T,T') were subjected to loading and at least 4 samples were tested in each direction and environmental condition. The shear strain and stress according to the direction (i,T'), where the direction i corresponds to the L or T material direction, were calculated as follows:

$$\varepsilon_{iT'} = \frac{\operatorname{atan}\left(\frac{u_i}{t}\right)}{2} = \frac{\gamma_{iT'}}{2} \quad (2)$$

$$\sigma_{iT'} = \frac{P_i}{Lb} \quad (3)$$

where u_i is the displacement of the material oriented along direction i and measured by the LVDT sensor, t is the thickness of the sample, $\gamma_{iT'}$ is the angular distortion in plan (i,T'), P_i is the load on the material oriented along direction i, L is the length of the sample and b is the width of the sample.

The shear moduli in each material direction were calculated using a linear regression on the shear strain/stress curve for a strain range between 0 and $1.5.10^{-3}$. The test was stopped once the specimen has broken slowly or the measuring range of the LVDT was reached.

Bonding conditions

The conditions for bonding the core materials to the metal parts as a function of the tested environmental conditions are summarized in Table 1. Concerning the thermocompression process, an Agila® Presse 100 kN machine was used. For the paper honeycomb, expanding/foaming adhesives have been used to provide a larger bonding surface. The bonding of the materials for mechanical testing under the EC2 environment was more difficult. It was necessary to ensure a high interlaminar strength between the metal plates and the core materials, while at the same time ensuring that no damage was caused by water desorption into the material itself.

The balsa wood was therefore bonded directly at condition EC2 using clamps. The rPET foam was first conditioned under condition EC2, then bonded and finally conditioned again under condition EC2. The honeycomb was bonded

using thermocompression under condition EC2. Just before the beginning of the mechanical test, the paper-based material was conditioned under the environment EC2 until the EMC was reached.

2.2.2 Creep shear tests

The time-delayed behaviour of the core materials was investigated under condition EC1 for different stress levels below and above or close to the yield stress: (i) 1 and 0.5 MPa for the balsa wood, (ii) 0.27 and 0.15 MPa concerning the paper honeycomb and (iii) 0.4 and 0.2 MPa about rPET foam. This behaviour was also studied under environment EC2 and compared to that obtained at EC1 only for the stress at 0.5 MPa, 0.15 MPa and 0.2 MPa. The same machine and shear assembly as for the monotonic tests was used. The load path was divided into two parts: one hour of creep and one hour of recovery. The PMMA box and the Inec 70-90 relative humidity generator were also used to maintain the two studied environmental conditions with temperature and relative humidity variations of ±3 °C and ±5%, respectively, during the creep/recovery test. The bonding conditions of the core materials were the same as those for the monotonic tests. Materials were solicited along the stiffer material direction: L-direction for the balsa wood and the paper honeycomb, T-direction concerning the rPET foam. For each material and environmental condition, the creep/recovery tests were realized on 3 samples. Some parameters were extracted from the time/strain and strain/stress curves (Figure 3):

- the instantaneous shear strain ε_{ins} obtained when the nominal stress is reached for the first time,
- the instantaneous shear modulus G_{ins} measured between zero strain and $1.5.10^{-3}$ strain,
- the maximum shear strain ε_{max},
- the secondary creep stage strain rate $\dot{\varepsilon}_{creep}$ determined in a range of times between 2000 s and 3500 s,
- the time delayed strain during the creep stage ε_{delc} defined as the difference between ε_{max} and ε_{ins},
- the residual shear strain ε_{res} corresponding to the shear strain at the end of the creep/recovery test,
- the time delayed strain during the recovery stage ε_{delr} defined as the difference between the shear strain once the recovery stage begins and ε_{res}.

2.3 Identification of the viscoelastic properties

2.3.1 Viscoelastic model

A 3D model was used to study the viscoelastic behaviour of the core materials based on the formulation of Boubakar *et al.* [47]. The viscoelastic flow $\underline{\dot{\varepsilon}}^{ve}$ is defined as the sum of the elementary viscoelastic flows $\underline{\dot{\xi}_i}$ (see

Eq. 4). The number of viscoelastic mechanisms (labelled N) is chosen empirically at 31. It allows to accurately describe the viscoelastic behaviour of cellulose based materials as shown in [48].

$$\underline{\dot{\varepsilon}}^{ve} = \sum_{i=1}^{N} \underline{\dot{\xi}_i} = \sum_{i=1}^{N} \frac{1}{\tau_i} (\mu_i \underline{\underline{S_{ve}}}\,\underline{\sigma} - \underline{\xi_i}), \tag{4}$$

The expression of the i[th] elementary viscoelastic flow is given by the following equation:

$$\underline{\dot{\xi}_i} = \frac{1}{\tau_i} (\mu_i \underline{\underline{S_{ve}}}\,\underline{\sigma} - \underline{\xi_i}), \tag{5}$$

where τ_i and μ_i are the release time and the weighting coefficient of the i[th] elementary viscous mechanism, respectively. The viscoelastic compliance tensor is $\underline{\underline{S_{ve}}}$ and $\underline{\sigma}$ is the Cauchy stress tensor.

Considering an orthotropic material, the viscoelastic compliance can be written as follows:

$$\underline{\underline{S_{ve}}} = \begin{bmatrix} \frac{\beta_L}{E_L} & -\beta^*_{LT}\frac{\nu_{LT}}{E_L} & -\beta^*_{LT'}\frac{\nu_{LT'}}{E_L} & 0 & 0 & 0 \\ -\beta^*_{LT}\frac{\nu_{LT}}{E_L} & \frac{\beta_T}{E_T} & -\beta^*_{TT'}\frac{\nu_{TT}{}'}{E_T} & 0 & 0 & 0 \\ -\beta^*_{LT'}\frac{\nu_{LT'}}{E_L} & -\beta^*_{TT'}\frac{\nu_{TT}{}'}{E_T} & \frac{\beta_{T'}}{E_{T'}} & 0 & 0 & 0 \\ 0 & 0 & 0 & \frac{\beta_{LT}}{G_{LT}} & 0 & 0 \\ 0 & 0 & 0 & 0 & \frac{\beta_{LT'}}{G_{LT'}} & 0 \\ 0 & 0 & 0 & 0 & 0 & \frac{\beta_{TT'}}{G_{TT'}} \end{bmatrix}$$

where $\beta_L, \beta_T, \beta_{T'}, \beta^*_{LT}, \beta^*_{LT'}, \beta^*_{TT'}, \beta_{LT}, , \beta_{LT}$ and $\beta_{TT'}$ are the viscous parameters that characterize the viscosity of the material, E_i is the elastic moduli in each material direction; and ν_{ij} and G_{ii} are the Poison's ratios and shear moduli within the plane (i,j).

This viscoelastic model has the peculiarity of linking the logarithm of the release times to the weighting coefficients of the viscous mechanisms by a Gaussian distribution defined by its mean noted $\ln(\tau_1)$ and its standard deviation (SD).

2.3.2 Identification of the model parameters

The identification of the viscoelastic parameters was carried out on the recovery part of the test. Although the viscoelastic behaviour can be affected by the creep stage, the method used in this work however excludes the irreversible mechanisms that can be expressed in this phase of the loading, particularly during tests in harsh environments. The recovery stage was considered to start once the load is null.

Only three parameters remain to be identified when one considers a one-dimensional shear loading: the viscous parameter $\beta_{LT}{}'$ ($\beta_{TT}{}'$ for rPET foam), the mean and the standard deviation of the Gaussian distribution of the elementary viscoelastic components. The two previous parameters and the term $\frac{\beta_{LT\prime}}{G_{LT\prime}}$ ($\frac{\beta_{TT\prime}}{G_{TT\prime}}$ for rPET foam) have been identified using an inverse method applied to the viscoelastic compliance during the recovery stage. The viscous parameter was then calculated by measuring the modulus during the unloading between $\varepsilon_{\max}$ and $\varepsilon_{\max} - 1.5.10^{-2}$. The optimization algorithm used in this work adopts a genetic algorithm and a Levenberg–Marquardt algorithm to avoid early convergence to a local minimum. All these tools are already implemented in the free software MIC2M [49] used in this study.

3 RESULTS AND DISCUSSION

3.2 Density and moisture content

The density of the cores at 23 °C-50% RH and the EMC under conditions EC1 and EC2 are shown in Table 2. The densities of the balsa wood panel, the paper honeycomb and the rPET foam are 97 kg.m^{-3}, 47 kg.m^{-3} and 80 kg.m^{-3}, respectively. These values are in accordance with the data provided by the suppliers. The distribution of the density values of the balsa wood is the most scattered. This can be explained by the fact that the latter is composed of an assembly of balsa blocks. Balsa wood and paper honeycomb have a larger water content under ambient conditions than rPET. The EMC under environment EC1 is equal to 9.2%, 7.3% and 0.66% for the balsa wood panel, paper honeycomb and rPET foam, respectively. The three materials present different moisture sorption mechanisms. In the paper honeycomb, several moisture diffusion mechanisms occur: (i) diffusion of water vapour through the empty space between the fibres, (ii) diffusion into small pores, (iii) diffusion within the wood fibres [50]. The sorption of water in the balsa wood panel is principally due to the hydrophilic constituents of the fibre cell wall [51]. In the case of the petroleum-based material, water penetrates the PET by forming hydrogen bonds with polar ester groups. The number of hydrogen bonds are then reduced and the relaxation of the main chain become so easier [52]. The direct consequence is the glass transition temperature decreases so with the increase of water content [53,54]. For a very long time of exposure, the water can cause the hydrolysis of the material by cutting the chains of ester functions[55,56]. The diffusion kinetics is influenced by the average molecular weight of the polyester chains, by the orientation of these chains and also by the crystallinity of the material [55,56]. Under the environmental conditions EC2, a small decrease in the EMC is observed for the balsa wood and the paper honeycomb with mean values of 7.4% and 6.0% respectively. These results are in accordance with the sorption curves of wood [57]. For the rPET, the EMC increases to a mean value of 0.76%. Therefore, the main

difference induced by the two conditioning conditions in the materials is primarily due to the temperature, since the moisture content remains slightly lower or higher, depending on the core material considered.

3.3 Monotonic and creep behaviour under ambient conditions

Monotonic behaviour

The monotonic shear behaviour of the core materials and the associated mechanical properties are presented in Figure 4 and in Figure 5 for the (L,T') and (T,T') shear planes under environment EC1. The mean values of the shear modulus according to the (L,T') shear plane are measured at 123 MPa, 49 MPa and 18 MPa for the balsa wood panel, paper honeycomb and rPET foam, respectively. These values are in accordance with those provided in the technical datasheet [28,58]. The specific shear modulus of the balsa wood panel, paper honeycomb and rPET foam are measured at 1,27 $MPa.kg^{-1}.m^3$, 1,04 $MPa.kg^{-1}.m^3$ and 0,23 $MPa.kg^{-1}.m^3$ respectively. In comparison, the specific moduli of PVC and PUR foam are equal to 0,37 $MPa.kg^{-1}.m^3$ and 0,09 $MPa.kg^{-1}.m^3$, respectively [35,59]. The values of the shear modulus of the balsa wood panel and the paper honeycomb are 1.5 and 3.8 times higher according to the (L,T') shear plane than to the (T,T') plane, respectively. This difference was already observed on balsa wood in the literature [30]. The maximum shear stress also depends on the loading planes, with a strength 1.6 times higher in the (L,T') shear plane than in the (T,T') plane for balsa wood. Concerning the paper honeycomb, the strength is 2.2 times higher in the (L,T') shear plane than in the (T,T') plane. The shear strength of the balsa is significantly higher than that of the other core materials. For the rPET foam, the shear modulus and strength are similar in the two planes.

Figure 5 presents the evolution of the apparent shear modulus as a function of the stress for each material according to the two studied shear planes. The behaviour of the materials is nonlinear. After a first phase in which the apparent rigidity is almost constant or marked by a slight decrease, a clear break in slope is observed. The yield stresses according to the shear planes (L,T') and (T,T') are measured at approximately 1 and 0.5 MPa for the balsa wood panel, respectively, 0.3 and 0.15 MPa for the paper honeycomb and 0.3 MPa in both plane for the rPET foam. After the yield point, the apparent shear modulus decreases progressively due to damage propagation. Figure 4 shows damage phenomena such as shear buckles or deflection of honeycomb cells as already seen in the work of Pohl [43]. The failure of the rPET and balsa panel is initiated by the appearance of cracks at 45°.

Time-delayed behaviour

The time-delayed behaviour of the core materials is evaluated by using creep/recovery tests under ambient environment (23 °C-50% RH). Stress levels below and above (or close) the yield points have been here considered.

Figure 6 presents the viscoelastic compliance (defined as the ratio between the time-delayed angular distortion and the nominal shear stress) during the creep stage. Under constant loading, the deformation of the material increases rapidly, at first. This phase is generally called the primary creep stage for viscoelastic materials. This is followed by a secondary creep phase characterized by an almost constant strain rate. For the rPET and balsa wood panels, the viscoelastic compliance varies as a function of the stress level. Regardless of the shear stress level, the balsa wood panel presents the lowest time-delayed strain levels with viscoelastic compliance at the end of the creep stage equal to $1.1.10^{-3}$ and $2.4.10^{-3}$ MPa^{-1} for a shear stress of 0.5 MPa and 1 MPa, respectively. rPET exhibits a less pronounced time-delayed behaviour when subjected to a load lower than the yield stress (0.3 MPa) with a viscoelastic compliance equal to $5.1.10^{-3}$ MPa^{-1} at 0.2 MPa compared to $20.4.10^{-3}$ MPa^{-1} at 0.4 MPa. The time-delayed behaviour of the paper honeycomb is quite similar regardless of the level of solicitation. Although lighter than the other core materials (see Table 2), the paper honeycomb has the highest time-delayed strain under creep solicitation. The viscoelastic compliance at the end of the creep stage is equal to $34.8.10^{-3}$ MPa^{-1} and $28.9.10^{-3}$ MPa^{-1} at 0.27 and 0.15 MPa, respectively.

Other features were also extracted from the creep/recovery tests. They are synthetized in Table 4, Table 5 and Table 6 for the balsa wood, the paper honeycomb and the rPET foam, respectively. The irreversible nature of the behaviour is more pronounced in the paper honeycomb samples. For a nominal stress corresponding to 38% of the quasi-static shear strength, the residual strain is equal to $1.1.10^{-3}$ against $1.2.10^{-4}$ for the rPET and the balsa wood panel, respectively, both subjected to a 36% of the quasi-static shear strength. For the wood and foam samples, the instantaneous shear modulus is of the same order of magnitude as the one determined during the quasi-static tests. In contrast, for paper honeycomb samples, the instantaneous modulus (measured during the loading phase of the creep stage) is approximately 22% higher than the elastic modulus measured during the quasi-static tests. This is due to the difference in loading rate between the two experiments (0.03 $MPa.s^{-1}$ for quasi-static tests against 0.14 $MPa.s^{-1}$ for creep/recovery test). This feature also highlights the strong dependence of the paper honeycomb on the loading rate.

The results also show that the strain rate in the secondary creep stage ($\dot{\varepsilon}_{creep}$) increases with the stress level. For paper honeycomb, it is twice as high at 0.27 MPa than it is at 0.15 MPa. Regardless of the material, the time delayed strain during the creep stage is higher than that measured during the recovery stage, therefore indicating the presence of an irreversible mechanism, such as damage and deformation (collapse and buckles of cell units), during the creep part. For balsa, the time delayed strain is twice larger during creep than under recovery.

3.4 Impact of severe environmental conditions on the monotonic shear behaviour

The monotonic shear behaviour of the core materials is also studied under the more severe hygrothermal condition, EC2. The stress-strain curves and the failure profiles along the shear planes (L,T') and (T,T') are presented in Figure 7. The evolution of the tangent shear modulus as a function of the stress is given in Figure 8. The quasi-static behaviour of all the core materials is first linear until a yield stress, whose values are shown in Table 7. The tangent shear modulus then decreases until the failure of the specimen. Compared to environmental conditions EC1, a decrease in the yield stress is also observed. In particular, the yield stress of the balsa core is 40% and 30% lower under the severe environment in the shear planes (L,T') and (T,T'), respectively. The evolution of the stress as a function of the strain is like the one observed under ambient conditions. The failure profiles are presented in Figure 7. The shear failures of the paper honeycomb samples are identical to those obtained at room temperature. Although cracks at 45° appear, the failure of the balsa is also due to the detachment of the balsa blocks glued together by a polyvinyl acetate base adhesive [30]. Concerning the rPET foam, the samples tested in the plan (L,T') do not present cracks as under ambient conditions. The tests are stopped due to the detachment of the material from the metal parts and, for one sample, due to the limit measure of the LVDT sensor. The detachment of the sample is also observed in the other shear plane. For the sample with the highest maximum stress, a crack at 45° is responsible for the failure. On the basis of these observations, the measured maximum stress thus gives the load threshold that should not be exceeded before skin/core separation and/or core failure in a sandwich structure consisting of an rPET foam core. According to the shear plane (L,T'), the shear modulus of balsa, paper honeycomb and rPET is measured at 88 MPa, 31 MPa and 10 MPa respectively. The shear stiffness is therefore 28%, 37% and 50% lower than that in the ambient environment. For the other shear planes, this decrease is 38%, 86% and 37% for the wood, honeycomb and foam, respectively. Considering that the moisture content in the core materials (see Table 2) is not very different under environments EC2 and EC1, the decrease in the shear stiffness is assumed to be mainly related to the temperature variation. For balsa wood, the mechanical properties of the material are mainly driven by the S2 layer of the cell wall, which is made up of cellulose microfibrils embedded in a matrix of lignin and hemicelluloses [31]. The decrease in the shear properties of the balsa wood panel under environment EC2 is attributed to the softening of the hemicellulose at 70°C due to the changes from a rigid to a viscous state [60]. The decrease in stiffness of the paper honeycomb is principally due to the activation of the viscoelastic properties of the paper constituents by temperature. The values of modulus measured for the rPET are in accordance with those measured by Garrido *et al.* [33]. Additionally, the decrease in this property, compared to ambient conditions, is due to (i) the plasticization of the polymer by the water molecule causing a decrease in the

glass temperature transition [56,61] and (ii) a glass transition temperature of PET close to 70 °C [53,54]. A decrease in the maximum shear stress is also observed for the core materials under a more severe environment. In particular, the shear stress for the balsa samples on the (L,T) plane is 30% lower at 23 °C than at 70 °C. Conversely, for this material, the strain at failure is twice as high

3.5 Impact of severe environmental conditions on the creep shear behaviour

The time-delayed behaviour of the three core materials is also investigated under the environmental conditions EC2. Figure 9 shows the evolution of the shear strain of the materials as a function of time during the creep/recovery test for the two studied environmental conditions. The mechanical characteristics are extracted from the raw experimental data and are shown in Table 4, Table 5 and Table 6 (balsa wood panel, paper honeycomb and rPET foam, respectively). As observed at ambient environment, the instantaneous shear modulus of the balsa wood panel and rPET foam is on the same order of magnitude as the one obtained from the quasi-static test. For the paper honeycomb, this engineering constant is higher than the one measured by the monotonic test. With the increase in severity of the environment, the irreversible character of the material is more pronounced. The residual shear strain is 5.3, 4.6 and 72 times higher than that at 23 °C for the balsa, paper honeycomb and rPET, respectively. Additionally, the time-delayed strains of the balsa wood panel, paper honeycomb and rPET foam determined during the recovery stage are 41%, 69% and 25% lower than those obtained during creep, respectively. For the same stress level, the maximum and the time-delayed strains during creep are larger under severe environment, regardless of the type of material considered. Specifically, for the balsa wood, these two mechanical parameters are twice and five times larger than those measured in ambient conditions, respectively. The strain rate related to the paper honeycomb during the secondary creep stage also appears to be higher at 70 °C, with a value equal to $3.1.10^{-7}$ s^{-1} at ambient environment and $7.1.10^{-7}$ s^{-1} in a severe environment. For the rPET foam, the decrease in the mechanical properties is explained by the fact that the temperature is close to the glass transition temperature. In view of the EMC decrease of the paper honeycomb and balsa wood under the EC2 environmental conditions (see Table 2), the decrease of the material the time-delayed behaviour is largely due to the higher temperature. Thus, the increase in the time-delayed strain can be explained by the activation of the viscoelastic properties of wood and paper with temperature [62]. Figure 10 represents the viscoelastic compliance of the core materials tested under the severe environment. The balsa wood allows a lower time-delayed strain compared to the other materials with a mean compliance value of $5.9.10^{-3}$ MPa^{-1}. The increase in the temperature on the rPET drastically increases the viscoelastic compliance with a value of $5.5.10^{-1}$ MPa^{-1} at 70 °C compared to $5.1.10^{-3}$ MPa^{-1} at 23 °C.

3.6 Viscoelastic behaviour

The previous paragraphs have described the mechanical behaviour of the different materials observed during the creep/recovery tests, which involve the presence of elasticity, viscoelasticity and irreversible mechanisms within the cores considered in this work. The present section focuses on the specific viscoelastic behaviour from the recovery phase. The identification of the 3D viscoelastic model parameters allows evaluating in details the influence of the stress level and the hygrothermal conditions on the viscoelastic behaviour of the cores. The identified parameters of the viscoelastic model are presented in Table 8 for all the core materials and tested stress levels in an ambient environment. The values of the cost function are comprised between 1.10^{-8} and 5.10^{-5}. The associated Gaussian distribution of the weighting parameters as a function of the release times for each sample of core materials is presented in Figure 11. For the balsa wood panel, the results highlight that two families of Gaussian distributions can be distinguished for the tested loading levels. The two populations are clearly linked to the stress level. The mixing of some curves owing to the same stress level between the two clusters is likely due to the variation of the yield stress as a function of the specimens cut in the balsa wood panel. Although a significant variation was measured from one sample to one another, the results show the robust dependence of the viscoelastic behaviour on the stress level [63]. The mean value of the logarithm of the release time is higher at 1 MPa than at 0.5 MPa. This means that the primary creep phase lasts longer at 1 MPa than at 0.5 MPa. Additionally, the shear viscous parameter is twice larger at 1 MPa than at 0.5 MPa.

Two different types of Gaussian distributions can also be observed in the case of the rPET foam with a mean value of the parameter $\ln(\tau_1)$ equal to 3.9 and 5.6 at 0.4 MPa and 0.2 MPa, respectively. As for balsa, the recovery viscoelastic behaviour of the rPET is characterised by one type of continuum spectrum for a stress level below the yield stress and another for a loading above this threshold. The viscous parameter is also more than twice higher for the stress level above the yield stress, than below. Opposite to the two other core materials, the viscoelastic behaviour of the paper honeycomb does not depend on the stress level. The values of the release time logarithm, rigidities and viscous parameter are similar for the different stress levels adopted. Moreover, all these parameters are larger than those of the rPET foam and the balsa wood panel. In particular, the shear viscous parameter is equal to 2.3 and 2.4 at 0.27 MPa and 0.15 MPa, respectively. Thus, the paper honeycomb is characterized by a higher viscoelastic strain than the other materials. The viscoelastic behaviour is also evaluated under the environmental conditions EC2. The identified model parameters are given in Table 9. The associated Gaussian distribution of the weighting parameters as a function of the release times for each sample of core materials is given in Figure 12.

For all the materials, the value of the shear viscous parameter increases with the severity of the environmental conditions. This material parameter is 5.4 higher than the one at ambient environment for the balsa wood panel, and even goes from a value of 0.06 to 3.28 in the case of the rPET foam. The Gaussian spectra are plotted in Figure 11 and compared with those obtained at EC1. Interestingly, when the wood is solicited at 0.5 MPa and the foam at 0.2 MPa, the Gaussian distributions at EC2 are similar to those at EC1 at 1 MPa for the balsa and 0.4 MPa for the rPET. The two studied stress levels under the severe environment are above the yield stress, and it seems that the viscoelastic behaviour of the rPET and the balsa is characterised by one distribution of weighting coefficients as a function of relaxation times below the yield stress and another after.

In the case of paper honeycombs, the Gaussian distribution appears to be not dependent on the environmental conditions.

4 CONCLUSIONS

The present paper focuses on the influence of hygrothermal conditions on the creep/recovery shear behaviour of three eco-friendly core materials: balsa wood, paper honeycomb and rPET foam. The monotonic and time-delayed behaviour are first studied under an ambient environment (23 °C-50% RH) and then under a more severe environment (70 °C-65% RH). Finally, the viscoelastic behaviour of the materials is identified using a 3D anisotropic model from the recovery phase under the two studied hygrothermal conditions.

This study highlighted the following points:

- A change of the environment only leads to small water uptake in the rPET foam and a small decrease of the moisture content in the balsa wood and the paper honeycomb. The decrease in the mechanical properties is therefore attributed to the higher temperature associated to those environements.
- Under ambient conditions, the balsa wood panel is the core material with the highest shear modulus and strength. When the loading plane is the one with the largest stiffness, the paper honeycomb performs better than the rPET foam.
- At room temperature, the balsa wood panels exhibits the lower time-delayed shear strain. The creep behaviour of the balsa wood panel and the rPET foam is dependent on the stress level. For a solicitation below the yield stress, the viscoelastic compliance of the rPET foam is lower than that of the paper honeycomb.
- A decrease in shear modulus, yield stress and shear strength is observed under the more severe environment for the three different core materials. This decrease is more pronounced in the case of the rPET foam.

- The maximum shear strain, the time delayed strain and the residual strain increase for all the core materials considered with the severity of the hygrothermal conditions. In the case of the rPET, this decrease is attributed to the PET glass transition. For the case of the two biobased materials, the temperature increase induces the softening of the cell wall constituents, in particular the hemicelluloses.
- The balsa wood exhibits the best creep resistance under the two tested hygrothermal conditions. The level of residual strain of this material in particular is lower than the one of the other core materials.
- The viscoelastic material release times and the shear viscous parameter of the balsa wood and the rPET foam depend on the stress level and the hygrothermal conditions. In particular, the post-creep viscoelastic behaviour of these two materials is characterized by one distribution of the release times for stress levels below the yield stress, and another distribution for those above. Unlike the viscous parameter, the release times of the viscoelastic behaviour of the paper honeycomb are not dependent on the test stress levels and the environmental conditions.
- The post-creep viscoelastic behaviour of the paper honeycomb is characterised by a higher viscoelastic strain than the two other materials, due to the larger values of viscous parameters related to this biobased honeycomb.

Acknowledgements

The authors would like to acknowledge the funding received from the Bio Based Industries Joint Undertaking under the European Union's Horizon 2020 research and innovation program under grant agreement No 744349–SSUCHY project. The authors would also like to thank Armacell Company for providing the rPET foam. This work has also been supported by the EIPHI Graduate school (contract "ANR-17-EURE-0002").

REFERENCES

[1] Gay D, Hoa SV, Tsai SW. Composite materials: design and applications. Boca Raton, FL: CRC Press; 2003.

[2] Castanie B, Bouvet C, Ginot M. Review of composite sandwich structure in aeronautic applications. Compos Part C Open Access 2020;1:100004. https://doi.org/10.1016/j.jcomc.2020.100004.

[3] Vijaya Ramnath B, Alagarraja K, Elanchezhian C. Review on Sandwich Composite and their Applications. Mater Today Proc 2019;16:859–64. https://doi.org/10.1016/j.matpr.2019.05.169.

[4] Manalo A, Aravinthan T, Fam A, Benmokrane B. State-of-the-Art Review on FRP Sandwich Systems for Lightweight Civil Infrastructure. J Compos Constr 2017;21:04016068. https://doi.org/10.1061/(ASCE)CC.1943-5614.0000729.

[5] Aktay L, Johnson AF, Kröplin B-H. Numerical modelling of honeycomb core crush behaviour. Eng Fract Mech 2008;75:2616–30. https://doi.org/10.1016/j.engfracmech.2007.03.008.

[6] Baley C, Bourmaud A, Davies P. Eighty years of composites reinforced by flax fibres: A historical review. Compos Part Appl Sci Manuf 2021;144:106333. https://doi.org/10.1016/j.compositesa.2021.106333.

[7] Moudood A, Rahman A, Khanlou HM, Hall W, Öchsner A, Francucci G. Environmental effects on the durability and the mechanical performance of flax fiber/bio-epoxy composites. Compos Part B Eng 2019;171:284–93. https://doi.org/10.1016/j.compositesb.2019.05.032.

[8] Alsubari S, Zuhri MYM, Sapuan SM, Ishak MR, Ilyas RA, Asyraf MRM. Potential of Natural Fiber Reinforced Polymer Composites in Sandwich Structures: A Review on Its Mechanical Properties. Polymers 2021;13:423. https://doi.org/10.3390/polym13030423.

[9] Ávila de Oliveira L, Coura GLC, PassaiaTonatto ML, Panzera TH, Placet V, Scarpa F. A novel sandwich panel made of prepreg flax skins and bamboo core. Compos Part C Open Access 2020;3:100048. https://doi.org/10.1016/j.jcomc.2020.100048.

[10] Oliveira PR, May M, Panzera TH, Scarpa F, Hiermaier S. Improved sustainable sandwich panels based on bottle caps core. Compos Part B Eng 2020;199:108165. https://doi.org/10.1016/j.compositesb.2020.108165.

[11] Mancuso A, Pitarresi G, Tumino D. Mechanical Behaviour of a Green Sandwich Made of Flax Reinforced Polymer Facings and Cork Core. Procedia Eng 2015;109:144–53. https://doi.org/10.1016/j.proeng.2015.06.225.

[12] Sergi C, Tirillò J, Sarasini F, Barbero Pozuelo E, Sanchez Saez S, Burgstaller C. The Potential of Agglomerated Cork for Sandwich Structures: A Systematic Investigation of Physical, Thermal, and Mechanical Properties. Polymers 2019;11:2118. https://doi.org/10.3390/polym11122118.

[13] Le Duigou A, Deux J-M, Davies P, Baley C. PLLA/Flax Mat/Balsa Bio-Sandwich—Environmental Impact and Simplified Life Cycle Analysis. Appl Compos Mater 2012;19:363–78. https://doi.org/10.1007/s10443-011-9201-3.

[14] Monti A. Élaboration et caractérisation d'une structure composite sandwiche à base de constituants naturels. Université du Maine, 2015.

[15] Fletcher MI. Balsa—Production and utilization. Econ Bot 1951;5:107–25. https://doi.org/10.1007/BF02984770.

[16] Midgley SJ, Blyth M, Howcroft N, Midgley D, Brown A. Balsa: biology, production and economics in Papua New Guinea. Canberra: Australian Centre for International Agricultural Research; 2010.

[17] Borrega M, Ahvenainen P, Serimaa R, Gibson L. Composition and structure of balsa (Ochroma pyramidale) wood. Wood Sci Technol 2015;49:403–20. https://doi.org/10.1007/s00226-015-0700-5.

[18] Martínez-Garza C, Campo J, Ricker M, Tobón W. Effect of initial soil properties on six-year growth of 15 tree species in tropical restoration plantings. Ecol Evol 2016;6:8686–94. https://doi.org/10.1002/ece3.2508.

[19] Pflug J, Vangrimde B, Verpoest I, Vandepitte D, Britzke M, Wagenführ A. Continuously Produced Paper Honeycomb Sandwich Panels for Furniture Applications, Kassel (Germany): 2004, p. 10.

[20] Bitzer T. Honeycomb Technology. Dordrecht: Springer Netherlands; 1997. https://doi.org/10.1007/978-94-011-5856-5.

[21] Salavatian S, D'Orazio M, Di Perna C, Di Giuseppe E. Assessment of Cardboard as an Environment-Friendly Wall Thermal Insulation for Low-Energy Prefabricated Buildings. In: Sayigh A, editor. Sustain. Build. Clean. Environ., Cham: Springer International Publishing; 2019, p. 463–70. https://doi.org/10.1007/978-3-319-94595-8_39.

[22] Latka JF. Paper in architecture: Research by design, engineering and prototyping. Architecture and the Built environment. 2017.

[23] Vaccari M. Environmental Assessment of Cardboard as a Building Material. MSc in Energy Efficient and Sustainable Building. Oxfor Brookes University - School of Built Environment, 2008.

[24] CEPI Sustainability Report. Confederation of European Paper Industry; 2011.

[25] Plastics Europe, EPRO. Plastics – the Facts 2018: An analysis of European plastics production, demand and waste data. 2018.

[26] Chae Y. Current research trends on plastic pollution and ecological impacts on the soil ecosystem: A review. Environ Pollut 2018:9.

[27] Armacell. Life Cycle Assessment: PET foams. 2018.

[28] Armacell. Technical Datasheet Core GR 2020.

[29] 3A Core Materials. Technical Data Sheet AIREX-T92 2018.

[30] Osei-Antwi M, de Castro J, Vassilopoulos AP, Keller T. Shear mechanical characterization of balsa wood as core material of composite sandwich panels. Constr Build Mater 2013;41:231–8. https://doi.org/10.1016/j.conbuildmat.2012.11.009.

[31] Borrega M, Gibson LJ. Mechanics of balsa (Ochroma pyramidale) wood. Mech Mater 2015;84:75–90. https://doi.org/10.1016/j.mechmat.2015.01.014.

[32] Da Silva A, Kyriakides S. Compressive response and failure of balsa wood. Int J Solids Struct 2007;44:8685–717. https://doi.org/10.1016/j.ijsolstr.2007.07.003.

[33] Garrido M, Correia JR, Keller T. Effects of elevated temperature on the shear response of PET and PUR foams used in composite sandwich panels. Constr Build Mater 2015;76:150–7. https://doi.org/10.1016/j.conbuildmat.2014.11.053.

[34] Sadler RL, Sharpe M, Panduranga R, Shivakumar K. Water immersion effect on swelling and compression properties of Eco-Core, PVC foam and balsa wood. Compos Struct 2009;90:330–6. https://doi.org/10.1016/j.compstruct.2009.03.016.

[35] Fathi A, Keller J-H, Altstaedt V. Full-field shear analyses of sandwich core materials using Digital Image Correlation (DIC). Compos Part B Eng 2015;70:156–66. https://doi.org/10.1016/j.compositesb.2014.10.045.

[36] Wu C, Vahedi N, Vassilopoulos AP, Keller T. Mechanical properties of a balsa wood veneer structural sandwich core material. Constr Build Mater 2020;265:120193. https://doi.org/10.1016/j.conbuildmat.2020.120193.

[37] Vahedi N, Wu C, Vassilopoulos AP, Keller T. Thermomechanical characterization of a balsa-wood-veneer structural sandwich core material at elevated temperatures. Constr Build Mater 2020;230:117037. https://doi.org/10.1016/j.conbuildmat.2019.117037.

[38] Bhangu SS. Effect of Moisture Absorption on the Mechanical Properties of Balsa Wood. ADFA J Undergrad Engeenering Res 2012;5:11.

[39] Stahlhut JA. Effect of Absorption of Liquids on the Mechanical Properties of Balsa Wood. ADFA J Undergrad Engeenering Res 2013;6:13.

[40] BASF. Green & Light and BASF developed Elastoskin® based paper honeycomb car trunk floor. BASF We Create Chem 2019. https://www.basf.com/global/en/media/news-releases/2019/02/p-19-135.html?WT.mc_id=P_135e.

[41] Chen Z, Yan N, Smith G, Deng J. Investigation of flexural creep of kraft paper honeycomb core sandwich panels using the finite element method. WOOD FIBER Sci 2012;44:10.

[42] Chen Z, Yan N. Investigation of elastic moduli of Kraft paper honeycomb core sandwich panels. Compos Part B Eng 2012;43:2107–14. https://doi.org/10.1016/j.compositesb.2012.03.008.

[43] Pohl A. Strengthened corrugated paper honeycomb for application in structural elements. ETH Zürich, 2009.

[44] ASTM International. C272/Test Method for Water Absorption of Core Materials for Structural Sandwich Constructions. 2001.

[45] ASTM International. D4442 - Test Methods for Direct Moisture Content Measurement of Wood and Wood-Based Materials. ASTM International; n.d. https://doi.org/10.1520/D4442-20.

[46] ASTM International. C273/Test Method for Shear Properties of Sandwich Core Materials. ASTM International; 2000. https://doi.org/10.1520/C0273_C0273M-19.

[47] Boubakar ML, Vang L, Trivaudey F, Perreux D. A meso–macro finite element modelling of laminate structures. Compos Struct 2003;60:275–305. https://doi.org/10.1016/S0263-8223(03)00012-6.

[48] Sala B, Gabrion X, Trivaudey F, Guicheret-Retel V, Placet V. Influence of the stress level and hygrothermal conditions on the creep/recovery behaviour of high-grade flax and hemp fibre reinforced GreenPoxy matrix composites. Compos Part Appl Sci Manuf 2021;141:106204. https://doi.org/10.1016/j.compositesa.2020.106204.

[49] Richard F. Identification du comportement et évaluation de la fiabilité des composites stratifiés. Université de Franche-Comté, 1999.

[50] Ramarao BV. Moisture sorption and transport processes in paper materials. Stud. Surf. Sci. Catal., vol. 120, Elsevier; 1999, p. 531–60. https://doi.org/10.1016/S0167-2991(99)80564-3.

[51] Jin F, Jiang Z, Wu Q. Creep Behavior of Wood Plasticized by Moisture and Temperature. BioResources 2015;11:827–38. https://doi.org/10.15376/biores.11.1.827-838.

[52] Chen Y, Lin Z, Yang S. Plasticization and Crystallization of Poly(ethylene Terephthalate) Induced by Water. J Therm Anal Calorim 1998;52:565–8. https://doi.org/10.1023/A:1010123723719.

[53] Chen D, Zachmann HG. Glass transition temperature of copolyesters of PET, PEN and PHB as determined by dynamic mechanical analysis. Polymer 1991;32:1612–21. https://doi.org/10.1016/0032-3861(91)90396-Z.

[54] Wang Y, Wang W, Zhang Z, Xu L, Li P. Study of the glass transition temperature and the mechanical properties of PET/modified silica nanocomposite by molecular dynamics simulation. Eur Polym J 2016;75:36–45. https://doi.org/10.1016/j.eurpolymj.2015.11.038.

[55] van Schoors LV. Vieillissement hydrolytique des géotextiles polyester (polyéthylène téréphtalate): Etat de l'art. Bull Lab Ponts Chaussées 2007:23.

[56] Jabarin SA, Lofgren EA. Effects of water absorption on physical properties and degree of molecular orientation of poly (ethylene terephthalate). Polym Eng Sci 1986;26:620–5. https://doi.org/10.1002/pen.760260907.

[57] Straube J, Onysko D, Schumacher C. Methodology and Design of Field Experiments for Monitoring the Hygrothermal Performance of Wood Frame Enclosures. J Therm Envel Build Sci 2002;26:123–51. https://doi.org/10.1177/0075424202026002098.

[58] 3A Composites Core Materials. Technical Datasheet Balsa SB 2016.

[59] Garrido M, Correia JR, Keller T. Effect of service temperature on the shear creep response of rigid polyurethane foam used in composite sandwich floor panels. Constr Build Mater 2016;118:235–44. https://doi.org/10.1016/j.conbuildmat.2016.05.074.

[60] Goodrich T, Nawaz N, Feih S, Lattimer BY, Mouritz AP. High-temperature mechanical properties and thermal recovery of balsa wood. J Wood Sci 2010;56:437–43. https://doi.org/10.1007/s10086-010-1125-2.

[61] Kamiya Y, Hirose T, Naito Y, Mizoguchi K. Sorptive dilation of polysulfone and poly(ethylene terephthalate) films by high-pressure carbon dioxide. J Polym Sci Part B Polym Phys 1988;26:159–77. https://doi.org/10.1002/polb.1988.090260109.

[62] Placet V, Passard J, Perré P. Viscoelastic properties of green wood across the grain measured by harmonic tests in the range 0–95°C: Hardwood vs. softwood and normal wood vs. reaction wood. Holzforschung 2007;61:548–57. https://doi.org/10.1515/HF.2007.093.

[63] Reichel S, Kaliske M. Hygro-mechanically coupled modelling of creep in wooden structures, Part I: Mechanics. Int J Solids Struct 2015;77:28–44. https://doi.org/10.1016/j.ijsolstr.2015.07.019.

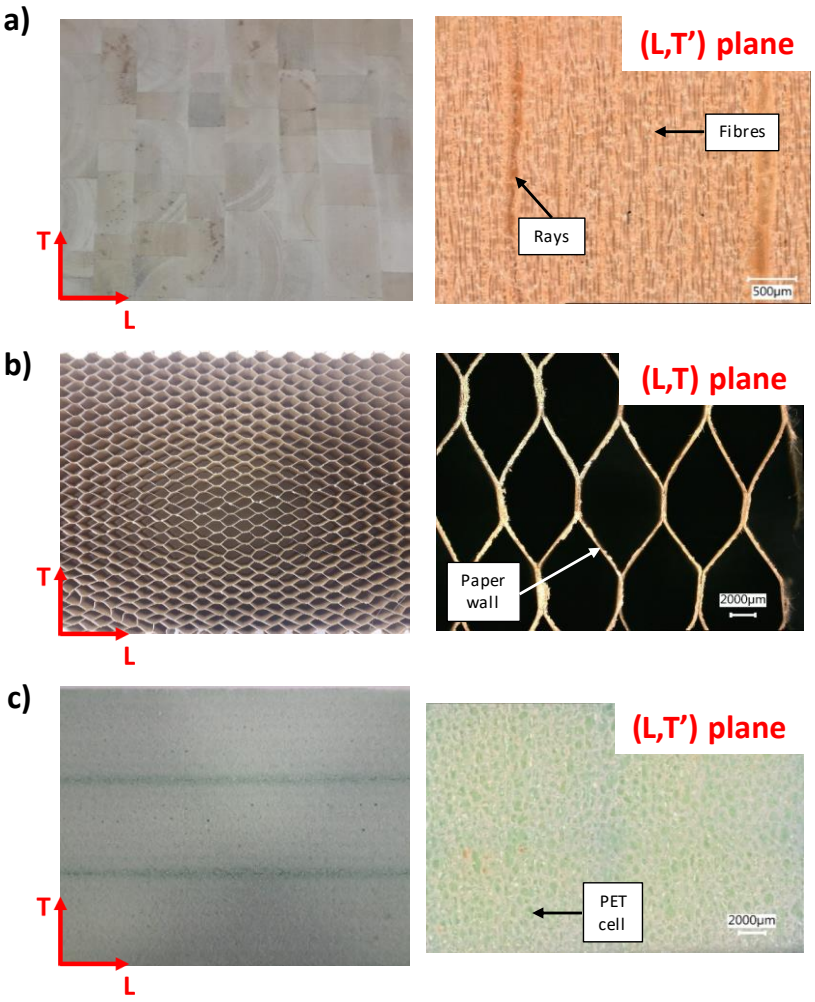

Figure 1. Images of the balsa wood a), paper honeycomb b) and rPET foam c) at a macroscopic scale (left column), with their associated coordinate systems, and at microscopic scale following the plane (L,T') or (L,T) (right column)

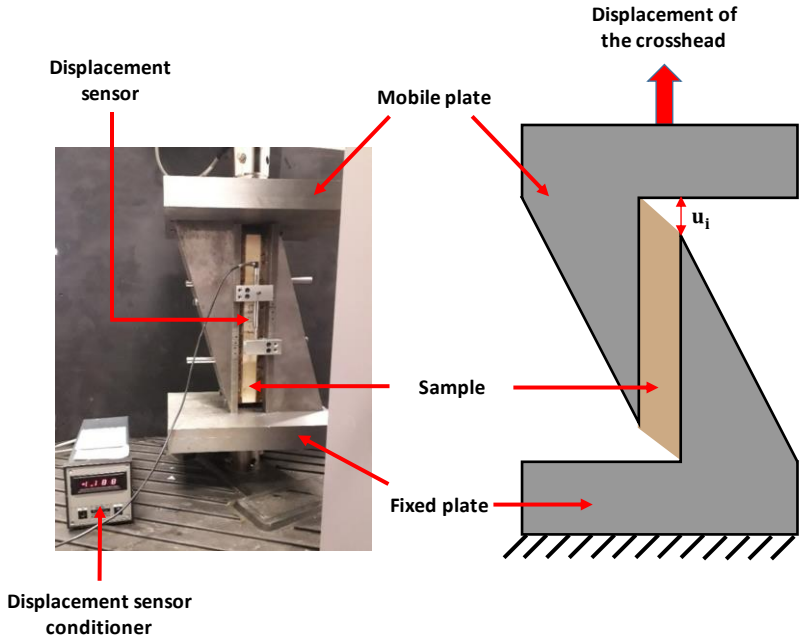

Figure 2. Transverse shear test rig installed on the tensile testing machine

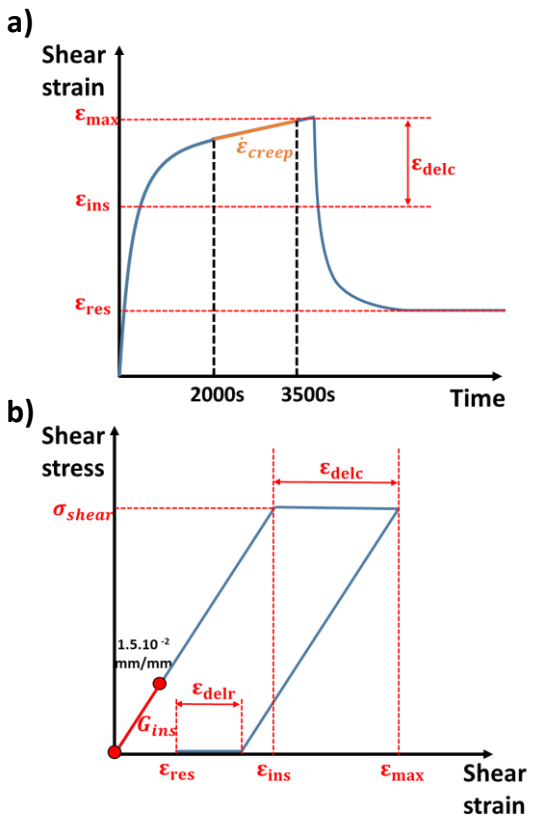

Figure 3. Parameters identified from the time/strain a) and the strain/stress b) representations

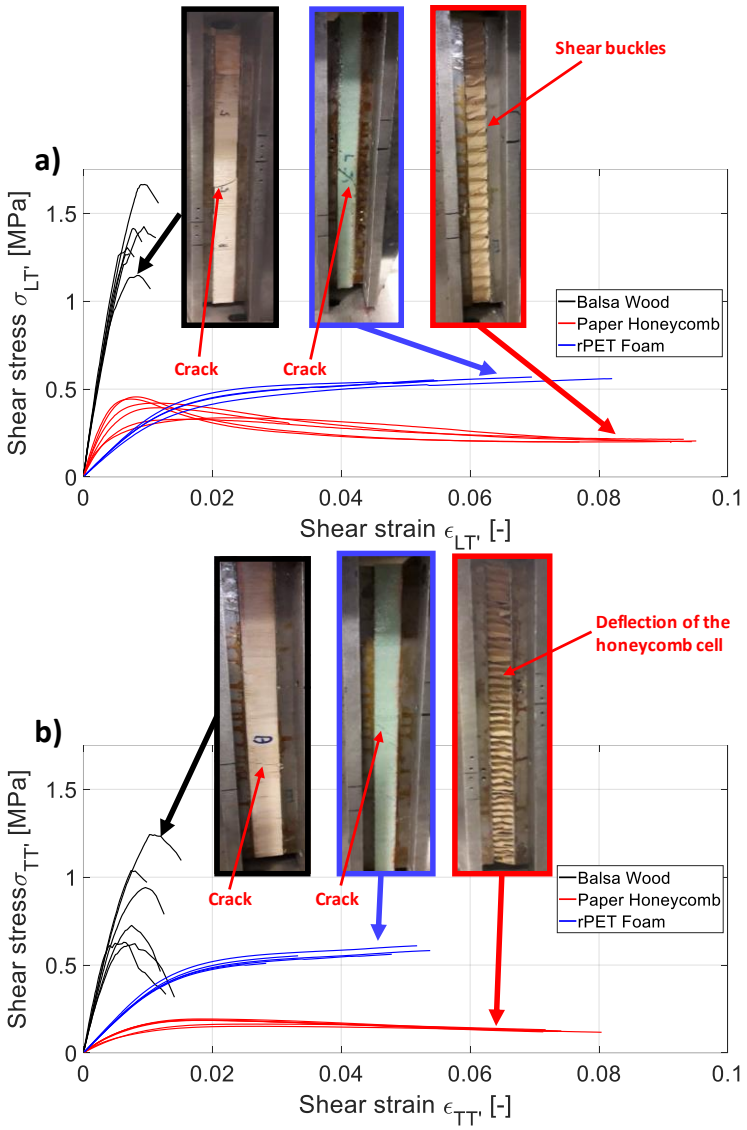

Figure 4. Shear stress-strain curves and failure profiles of the core materials subjected to shear in the shear planes (L,T') a) and (T,T') b) under the EC1 environmental conditions

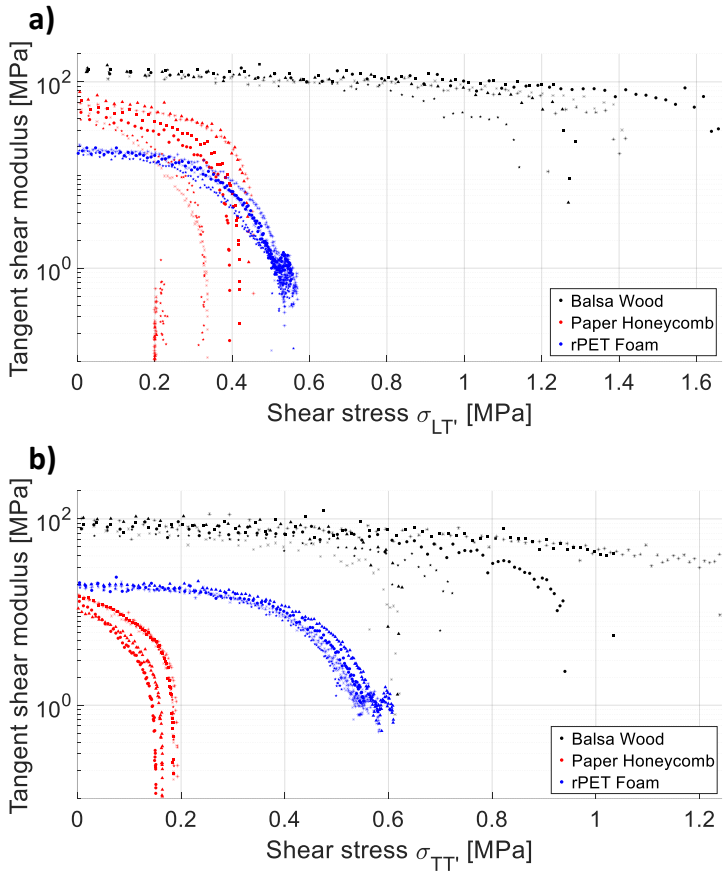

Figure 5. Evolution of the tangent shear modulus of the different core materials subjected to shear along the shear planes (L,T') a) and (T,T') b) in the EC1 environment

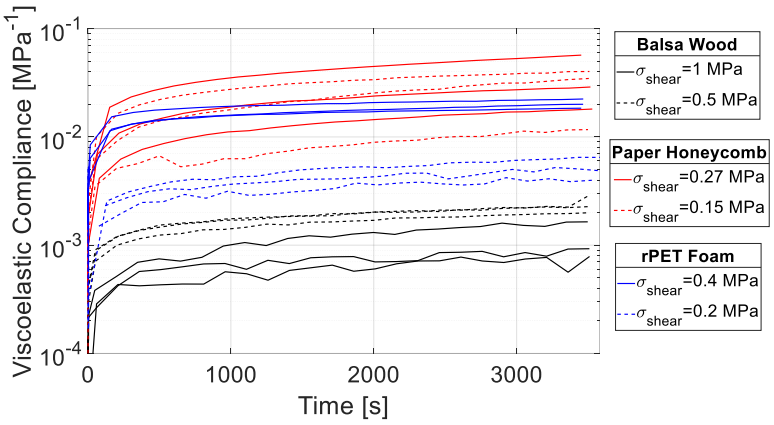

Figure 6. Evolution of the viscoelastic compliance as a function of creep time for the different core materials under the EC1 environment and various stress levels

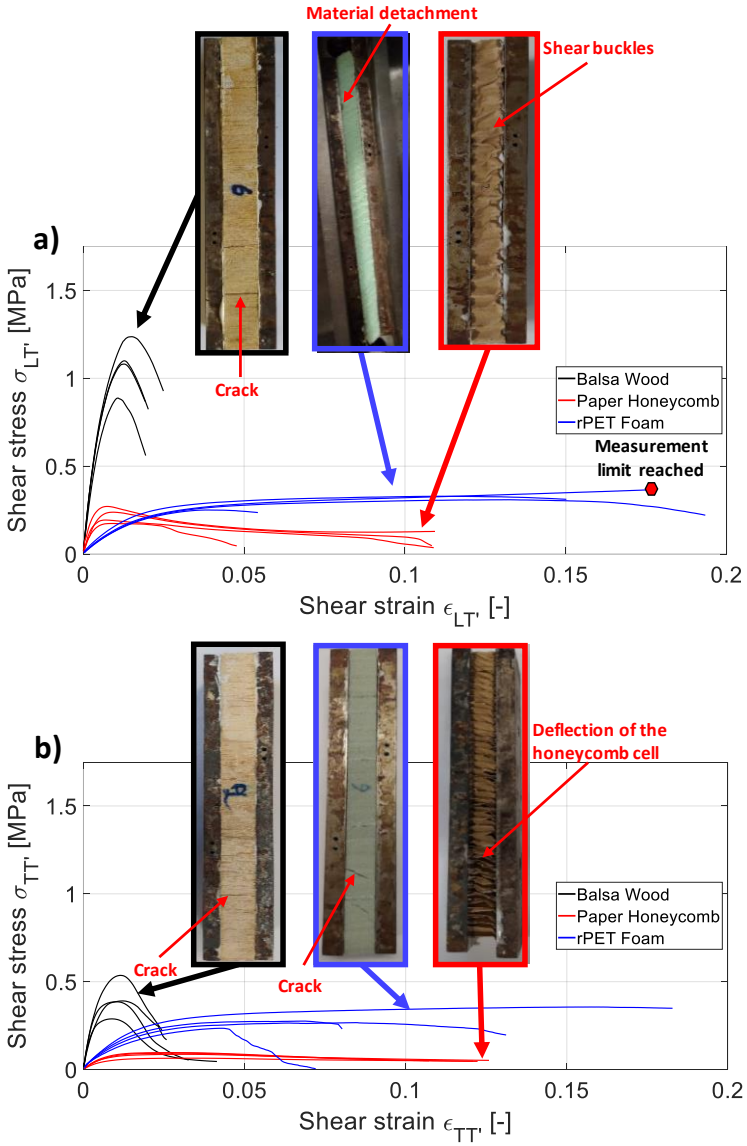

Figure 7. Shear stress-strain curves and failure profiles of the core materials subjected to shear along the shear planes (L,T') a) and (T,T') b) in the EC2 environmental conditions

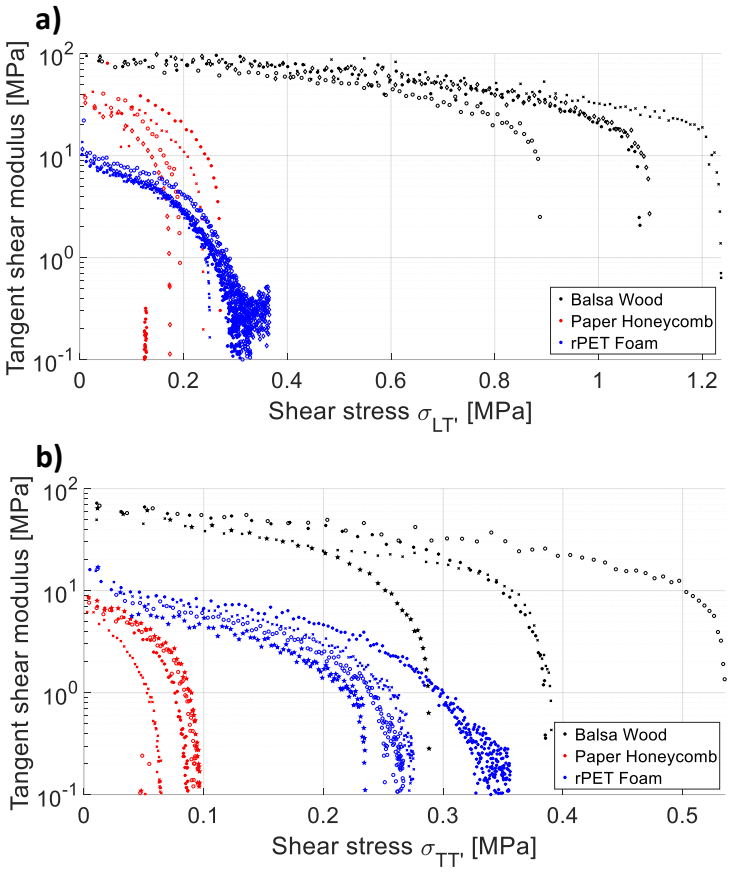

Figure 8. Evolution of the tangent shear modulus of the core materials subjected to shear along the shear planes (L,T') a) and (T,T') b) in the EC2 environment

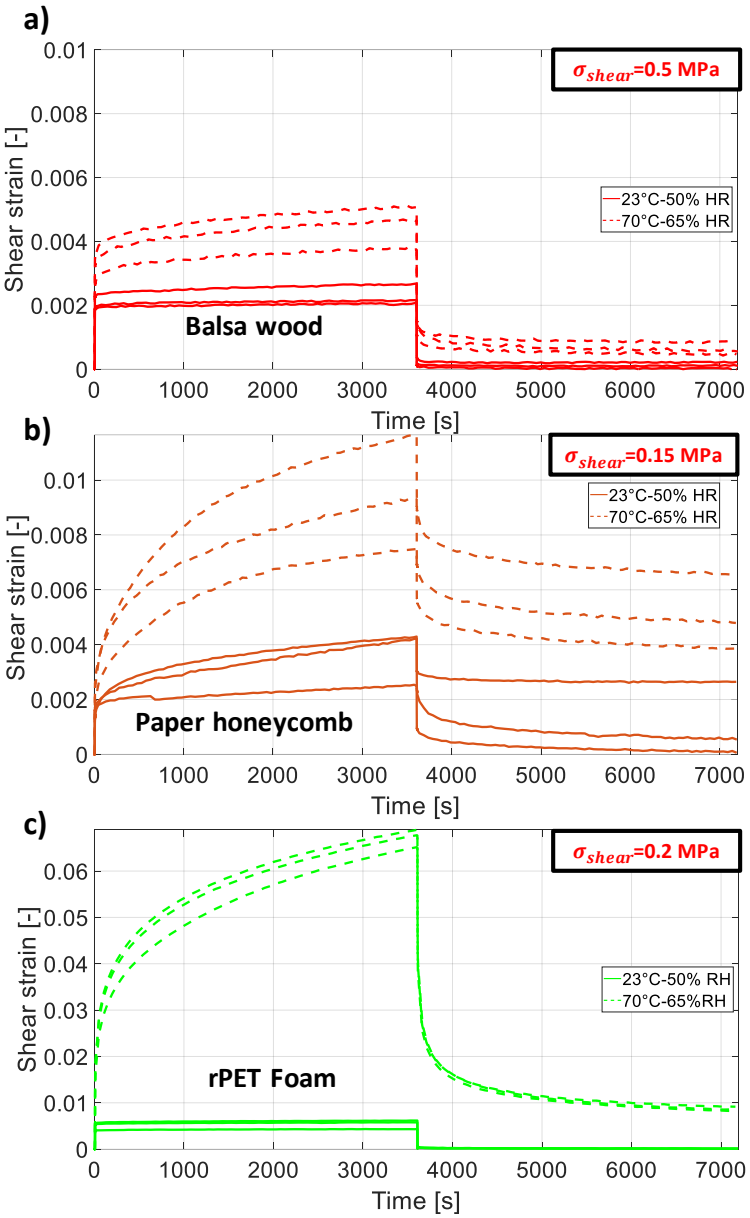

Figure 9. Creep/recovery behaviour of the balsa wood a), the paper honeycomb b) and the rPET foam c) subjected to nominal stresses of 0.5, 0.15 and 0.2 MPa, respectively, under environmental conditions EC1 and EC2

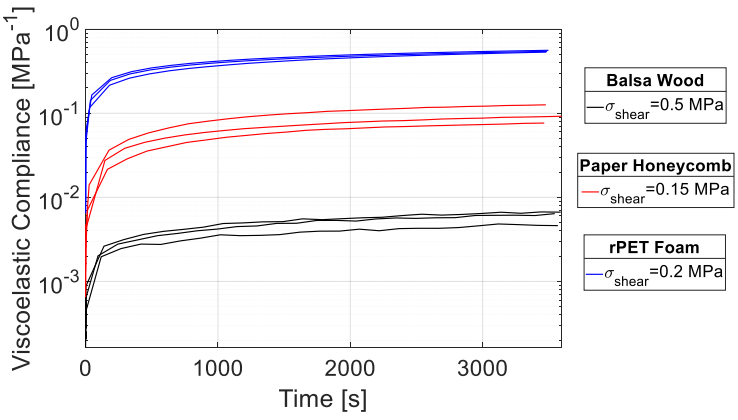

Figure 10. Viscoelastic creep compliance of all materials tested in the EC2 environment

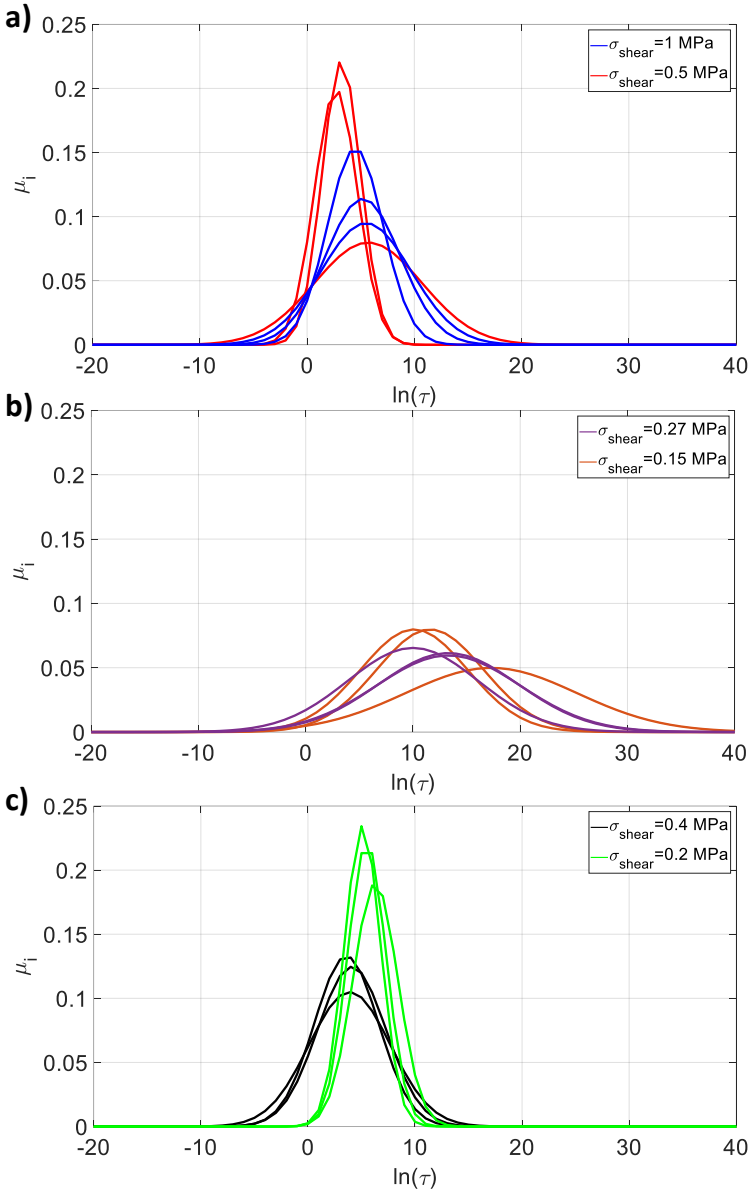

Figure 11. Gaussian distribution of the rigidities μ_i as a function of the logarithm of the released time ln(τ) identified from the recovery curve for different stress levels for balsa wood a), paper honeycomb b) and rPET foam samples c) solicited under environment EC1

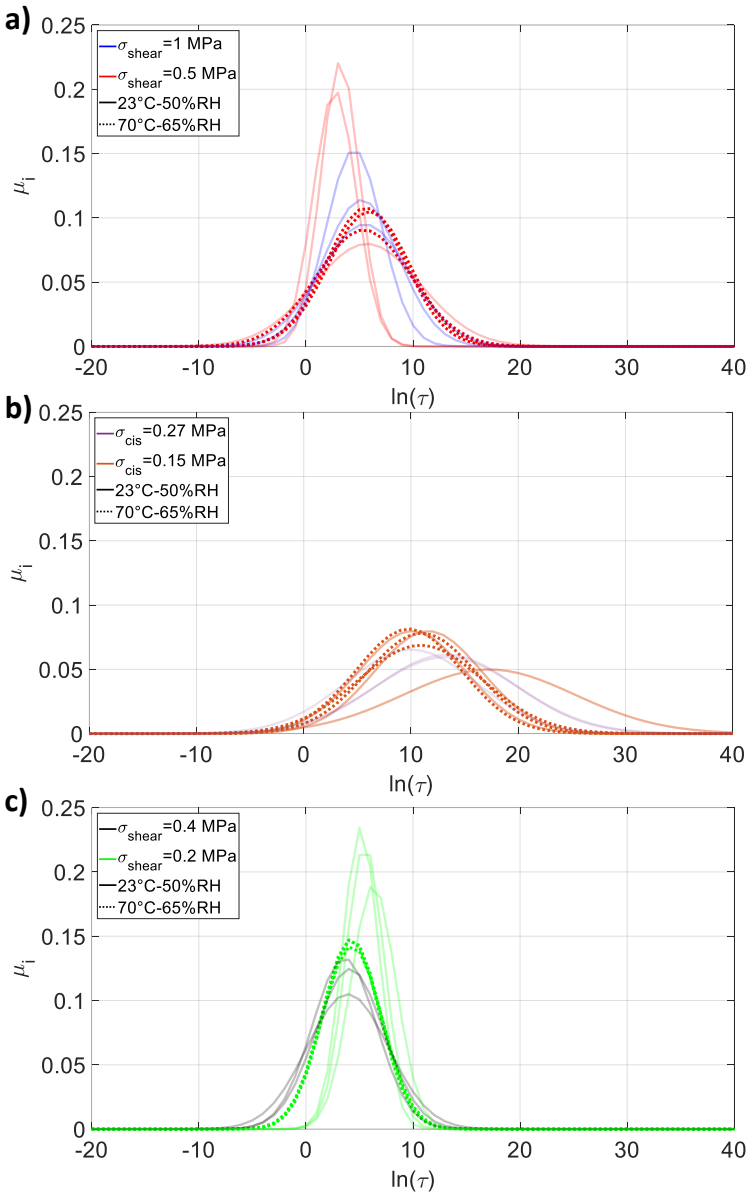

Figure 12. Comparison of the Gaussian distribution of the rigidities μ_i as a function of the logarithm of the released time ln(τ) identified from the recovery curve for different stress levels under environments EC1 and EC2 for balsa wood a), paper honeycomb b) and rPET foam samples c)

Table 1. Bonding conditions and adhesives selected for the different materials and environmental conditions

Material	Tests environmental conditions	Adhesives	Type of bonding
Balsa wood	EC1	Sicomin® GreenPoxy 56	Themocompression 1 h/130 °C/0.25 bar
	EC2	Epoxy® Loctite EA 9492	Bonding with clamps at least 24 h at 70 °C-65% RH
Paper honeycomb	EC1	Sader® expanding polyurethane glue	Bonding with clamps at least 48 h
	EC2	Sicomin® PB170	Themocompression 1 h/130 °C/0.25 bar
rPET foam	EC1	Sicomin® GreenPoxy 56	Themocompression 1 h/130 °C/0.25 bar
	EC2		Themocompression 1 h/80 °C/0.25 bar

Table 2. Density at 23 °C-50%RH and equilibrium moisture content under environmental conditions EC1 and EC2

Material	Density [kg.m^{-3}] at 23 °C – 50% RH	MC^{EC1} [%]	MC^{EC2} [%]
Balsa wood	97±6	9.2±0.1	7.4±0.1
Paper honeycomb	47±2	7.3±0.2	6.0±0.2
rPET foam	80±1	0.66±0.03	0.76±0.06

Table 3. Mechanical properties of core materials for shear solicitation according to the shear planes (L,T') and (T,T') under the EC1 environment (mean ± standard deviation)

Core material	**Shear plane**	**Shear modulus [MPa]**	**Max. shear stress [MPa]**	**Shear strain at failure/at maximum stress [10^{-3}.mm/mm]**	**Yield stress [MPa]**
Balsa wood	(L,T')	123±6	1.4±0.2	11±1/8.2±1.0	1
	(T,T')	81±9	0.9±0.3	14±2/8.3±1.5	0.5
Paper honeycomb	(L,T')	49±8	0.4±0.1	-/15±6	0.3
	(T,T')	13±1	0.18±0.02	-/21±5	0.15
rPET foam	(L,T')	18±1	0.56±0.01	65±13/65±13	0.3
	(T,T')	19±0.1	0.56±0.03	43±12/43±12	0.3

Table 4. Mechanical parameters identified from the creep/recovery tests at different stress levels on the balsa wood in the environmental conditions EC1 and EC2 (mean ± standard-deviation)

Stress level [MPa]	**1**	**0.5**	
Environmental condition	23 °C-50% RH (EC1)	23 °C-50% RH (EC1)	70 °C-65% RH (EC2)
G_{ins} [MPa]	119±8	126±11	92±13
$\varepsilon_{ins}.10^{-3}$ [-]	4.5±0.3	2.0±0.2	3.0±0.4
$\varepsilon_{delc}.10^{-3}$ [-]	1.2±0.3	0.3±0.2	1.5±0.2
$\varepsilon_{max}.10^{-3}$ [-]	5.8±0.6	2.3±0.3	4.6±0.6
$\dot{\varepsilon}_{creep}.10^{-7}$ [s^{-1}]	0.92±0.08	0.31±0.23	1.43±0.32
$\varepsilon_{delr}.10^{-3}$ [-]	0.63 ± 0.10	0.14 ± 0.02	0.88 ± 0.17
$\varepsilon_{res}.10^{-3}$ [-]	0.27 ± 0.19	0.12 ± 0.10	0.63 ± 0.18

Table 5. Mechanical parameters identified from the creep/recovery tests at different stress levels on the paper honeycomb in the environmental conditions EC1 and EC2 (mean ± standard-deviation)

Stress level [MPa]	**0.27**	**0.15**	
Environmental condition	23 °C-50% RH (EC1)	23 °C-50% RH (EC1)	70 °C-65% RH (EC2)
G_{ins} [MPa]	60±6	54±10	41±5
$\varepsilon_{ins}.10^{-3}$ [-]	2.4±0.2	1.5±0.2	2.1±0.3
$\varepsilon_{delc}.10^{-3}$ [-]	4.8±2.9	2.2±1.1	7.4±2.0
$\varepsilon_{max}.10^{-3}$ [-]	7.2±3.0	3.7±1.0	9.5±0.3
$\dot{\varepsilon}_{creep}.10^{-7}$ [s^{-1}]	6.2±4.4	3.1±1.5	7.1±2.1
$\varepsilon_{delr}.10^{-3}$ [-]	1.9 ±0.7	1.1±0.7	2.3±0.3
$\varepsilon_{res}.10^{-3}$ [-]	2.7 ± 2.0	1.1 ± 1.3	5.1 ± 1.4

Table 6. Mechanical parameters identified from the creep/recovery tests at different stress levels on the rPET foam in the environmental conditions at EC1 and EC2 (mean ± standard-deviation)

Stress level [MPa]	**0.4**	**0.2**	
Environmental condition	23 °C-50% RH (EC1)	23 °C-50% RH (EC1)	70 °C-65% RH (EC2)
G_{ins} [MPa]	19±0.2	20±1	11±0.2
$\varepsilon_{ins}.10^{-3}$ [-]	11.9±0.1	4.9±0.8	12.4±0.7
$\varepsilon_{delc}.10^{-3}$ [-]	4.1±0.4	0.58±0.08	55.3±1.4
$\varepsilon_{max}.10^{-3}$ [-]	16.0±0.5	5.5±0.9	67.7±2.0
$\dot{\varepsilon}_{creep}.10^{-7}$ [s^{-1}]	2.3±0.7	0.55±0.19	46.7±3.8
$\varepsilon_{delr}.10^{-3}$ [-]	1.6 ±0.2	0.46 ±0.08	41.4 ±1.6
$\varepsilon_{res}.10^{-3}$ [-]	1.29 ± 0.05	0.12 ± 0.02	8.6 ± 0.4

Table 7. Mechanical properties of core materials for shear solicitation according to the shear planes (L,T') and (T,T') under the EC2 environment (mean ± standard deviation)

Core material	**Shear plane**	**Shear modulus [MPa]**	**Max. shear stress [MPa]**	**Shear strain at failure/at maximum stress [10^{-3}.mm/mm]**	**Yield stress [MPa]**
Balsa wood	(L,T')	88±8	1.1±0.1	22±3/13±2	0.4
	(T,T')	51±6	0.4±0.1	11±1/31±8	0.2
Paper honeycomb	(L,T')	31±4	0.2±0.1	-/8±1	0.1
	(T,T')	7±1	0.09±0.01	-/31±3	0.05
rPET foam	(L,T')	10±1	0.30±0.04	-/94±49	0.15
	(T,T')	12±0.4	0.26±0.02	-/65±21	0.15

Table 8. Values of the viscoelastic model parameters identified from tests realized under environmental condition EC1 (mean ± standard deviation)

Core material	**Stress level [MPa]**	$\ln(\tau_1)$	**SD**	**Shear viscous parameter** ($\beta_{LT'}$ or $\beta_{TT'}$)
Balsa wood	1	5.1±0.5	3.4±0.8	0.15±0.03
	0.5	3.8±1.6	2.9±1.8	0.07±0.01
Paper honeycomb	0.27	12.2±1.9	6.4±0.3	2.3±0.3
	0.15	13.0±3.8	6.0±1.7	2.4±0.3
rPET foam	0.4	3.9±0.3	3.3±0.4	0.14±0.02
	0.2	5.6±0.6	1.9±0.2	0.06±0.01

Table 9. Values of the viscoelastic model parameters identified from tests realized under environmental condition EC2 (mean ± standard deviation)

Core material	**Stress level [MPa]**	$\ln(\tau_1)$	**SD**	**Shear viscous parameter** ($\beta_{LT'}$ or $\beta_{TT'}$)
Balsa wood	0.5	5.6±0.3	4.0±0.4	0.38±0.02
Paper honeycomb	0.15	10.6±0.6	5.3±0.5	3.18±0.42
rPET Foam	0.2	4.3±0.1	2.73±0.02	3.48±0.21